Projected heat stress under 1.5 °C and 2 °C global warming scenarios creates unprecedented discomfort for humans in West Africa

Mouhamadou Bamba Sylla, Aissatou Faye, Filippo Giorgi, Arona Diedhiou, Harald Kunstmann

Angaben zur Veröffentlichung / Publication details:

Sylla, Mouhamadou Bamba, Aissatou Faye, Filippo Giorgi, Arona Diedhiou, and Harald Kunstmann. 2018. "Projected heat stress under 1.5 °C and 2 °C global warming scenarios creates unprecedented discomfort for humans in West Africa." *Earth's Future* 6 (7): 1029–44. https://doi.org/10.1029/2018ef000873.

Earth's Future

RESEARCH ARTICLE
10.1029/2018EF000873

Projected Heat Stress Under 1.5 °C and 2 °C Global Warming Scenarios Creates Unprecedented Discomfort for Humans in West Africa

Mouhamadou Bamba Sylla[1], Aissatou Faye[1,2,3], Filippo Giorgi[2], Arona Diedhiou[4], and Harald Kunstmann[5]

[1]Competence Center, West African Science Service Center on Climate Change and Adapted Land Use, Ouagadougou, Burkina Faso, [2]International Centre for Theoretical Physics, Earth System Physics Section, Trieste, Italy, [3]Graduate Research Program on West African Climate System, West African Science Service Center on Climate Change and Adapted Land Use, Federal University of Technology, Akure, Akure, Nigeria, [4]University of Grenoble Alpes, IRD, CNRS, Grenoble INP, IGE, Grenoble, France, [5]Department of Atmospheric Environmental Research (IMK-IFU), Karlsruhe Institute of Technology, Institute of Meteorology and Climate Research, Garmisch-Partenkirchen, Germany

Key Points:
- Under 1.5 °C and 2 °C, Extreme Caution risk level becomes more extended and frequent, increasing the proportion of population in heat discomfort
- Days with dangerous heat stress risk emerge and prevail in the future causing everyone vulnerable to a likely heat cramp and heat exhaustion
- The higher level risk of heat stress and discomfort are more extended and more frequent in the 2 °C compared to the 1.5 °C warming scenario

Supporting Information:
- Supporting Information S1
- Data Set S1

Correspondence to:
M. B. Sylla,
syllabamba@yahoo.fr;
sylla.b@wascal.org

Citation:
Sylla, M. B., Faye, A., Giorgi, F., Diedhiou, A., & Kunstmann, H. (2018). Projected heat stress under 1.5 °C and 2 °C global warming scenarios creates unprecedented discomfort for humans in West Africa. *Earth's Future*, *6*, 1029–1044. https://doi.org/10.1029/2018EF000873

Received 22 MAR 2018
Accepted 3 JUL 2018
Accepted article online 9 JUL 2018
Published online 27 JUL 2018

Abstract Heat and discomfort indices are applied to the multimodel ensemble mean of COordinated Regional climate Downscaling EXperiment-Africa regional climate model projections to investigate future changes in heat stress and the proportion of human population at risk under 1.5 °C and 2 °C global warming scenarios over West Africa. The results show that heat stress of category Extreme Caution is projected to extend spatially (up to 25%) over most of the Gulf of Guinea, Sahel, and Sahara desert areas, with different regional coverage during the various seasons. Similarly, the projected seasonal proportion of human population at discomfort substantially increases to more than 50% over most of the region. In particular, in June–August over the Sahel and the western Sahara desert, new areas (15% of West Africa) where most of the population is at risk emerge. This indicates that *from 50% to almost everyone* over most of the Sahel countries and part of the western Sahara desert is at risk of *possible* heat cramp, heat exhaustion, and heat stroke in future climate scenarios. These conditions become more frequent and are accompanied by the emergence of days with *dangerous heat stress* category during which *everyone feels discomfort* and is vulnerable to a *likely* heat cramp and heat exhaustion. In general, all the above features are more extended and more frequent in the 2 °C than in the 1.5 °C scenario. Protective measures are thus required for outdoor workers, occupational settings in hot environments, and people engaged in strenuous activities.

1. Introduction

Climate change is causing warming over tropical Africa. Such temperature increase is expected to continue in the future with a projected global temperature change of about 1.4 °C to 4.8 °C (Intergovernmental Panel on Climate Change, 2014) and a regional response over the Sahel of about 2 °C to 6 °C (Sylla, Nikiema, et al., 2016) when considering the Representative Concentration Pathway 4.5 and 8.5 concentration scenarios (Moss et al., 2012). As a result, hot extremes will become more common and deadly in many regions across the world (Gasparrini et al., 2017; Im et al., 2017; Lee & Kim, 2016; Mora et al., 2017) and in tropical Africa (Giorgi et al., 2014; Liu et al., 2017; Russo et al., 2014), with their frequency, duration, and magnitude depending on the underlying forcing scenario (Anderson et al., 2018; Dosio, 2017; Linares et al., 2014; Russo et al., 2016). Such hot extremes can have widespread impacts on human and natural systems, thereby challenging the adaptive capacity and resilience of local populations and activities (Ceccherini et al., 2017; Fontaine et al., 2013; Pal & Eltahir, 2016; Sultan & Gaetani, 2016; Zougmoré et al., 2016).

In an effort to limit global warming, the international community reached an agreement at the United Nations Framework Convention on Climate Change 21st Conference of Parties held in Paris in 2015. This agreement sets the path to hold the global temperature increase below the 2 °C target, and possibly below a 1.5 °C target, with respect to preindustrial temperatures. While these global temperature limits are imperative for international negotiations, they do not explicitly consider regional changes. Furthermore, due to nonlinearities in the climate system, it is unreasonable to assume that all regional changes will be proportional to the mean global temperature change.

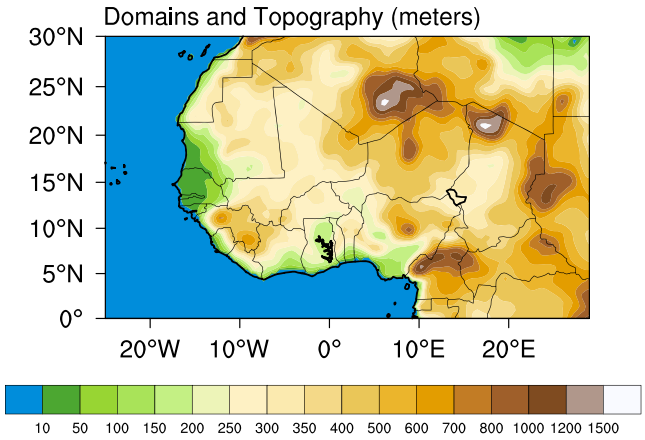

Figure 1. The West Africa domain of interest and its topography.

Therefore, in line with the Paris Agreement, the scientific community is increasingly interested in investigating the climate change impacts associated with the 0.5 °C difference between the two warming targets (i.e., 1.5 °C and 2 °C; James & Washington, 2013; Perkins-Kirkpatrick & Gibson, 2017; Schleussner et al., 2016). Despite the prominence of these two targets, only few studies have attempted to quantity the corresponding regional climate impacts over Africa. For example, a study by Schleussner et al. (2016) based on the Coupled Model Intercomparison Project Phase 5 global climate models (GCMs) found, among other results, an increase in the intensity of hot extremes (i.e., annual maximum value of daily maximum temperature) over tropical Africa. James et al. (2013) and Nikulin et al. (2018) analyzed ensembles of GCMs and regional climate models (RCMs), respectively, and found over continental Africa an increase in annual mean temperature characterized by strong regional heterogeneities between the subtropics and the coastal regions. More recently, Dosio et al. (2018) projected a significant increase of heat wave magnitude over this region even under the 1.5 °C target. Only few studies compared changes between the two warming targets with a focus over West Africa, but was limited to the issue of wet and dry spells (Klutse et al., 2018) and crop yields (Faye et al., 2018).

While these studies provided key information about increasing annual mean temperature and/or hot extremes for both warming scenarios, they did not provide direct information on comfort levels based on heat stress (since this must include information on humidity) that measures how hot the body really feels. During extremely hot and humid conditions, the body's ability to cool itself is challenged. Exposure to both high temperature and humidity generates occupational heat stress that can substantially affect people either working outdoors and in hot environments or engaged in physical activities (Lucas et al., 2014; Takahashi et al., 2007). This can undermine people's productivity and health, thus negatively impacting well-being and possibly the countries' economy (Chen et al., 2017; Kjellstrom et al., 2009; Liang et al., 2011). West Africa spans different climate zones with contrasting seasonal cycles (Diallo et al., 2014; Sylla, Elguindi, et al., 2016); it is densely populated, and it includes many economies in transition. Therefore, it can be particularly vulnerable to changes in heat stress. Information on projected heat stress can thus help policymakers to develop strategies for the most vulnerable areas aimed at protecting worker's health and productivity through mitigation and/or adaptation.

Based on these premises, in this study, we investigate the impacts of 1.5 °C and 2 °C global warming scenarios on heat indices over West Africa using a multimodel ensemble of 22 RCM simulations from the COordinated Regional climate Downscaling EXperiment (CORDEX; Giorgi et al., 2009; Giorgi & Gutowski Jr, 2015). CORDEX simulations have been already substantially validated over West Africa (Akinsanola et al., 2017; Dosio et al., 2015; Nikiema et al., 2017), and a central goal of this study is thus to examine the extent to which seasonal occurrences of different heat stress categories shift and spatially extend over the region. In particular, we also want to assess how changes in heat indices are translated into discomfort for local populations.

2. Data and Methodology

An ensemble of 22 simulations from the CORDEX-Africa experiments is used to assess the regional response of heat and discomfort indices under the 1.5 °C and 2 °C global warming scenarios over the West African domain shown in Figure 1.

The CORDEX RCMs along with the GCMs they downscaled, as well as the methodology to derive the 1.5 °C and 2 °C global warming scenarios, are reported in supporting information Tables S1 and S2. The model resolution is ~50 km (or ~1/2°), and the scenarios are derived as the 30-year period when the driving GCMs reaches 1.5 °C or 2 °C temperature increase compared to the reference period (see supporting information).

To assess the stress induced by the combined effects of high temperature and humidity, we apply the National Oceanic and Atmospheric Administration/National Weather Service heat index (hereafter referred as HI) formulation developed by Rothfusz (1990), which is given by the following equation (1):

Table 1
Summary of Heat Indices (HI), the Corresponding Risks Levels, and Heat Stress Classification, Along With the Health Problems They Can Trigger

HI (°F)	HI (°C)	Risk levels	Classification	Health problems
= < 80	= < 27	Extremely low	Safe	No significant stress
80–90	27–32	Low	Caution	Fatigue possible with prolonged exposure and/or physical activity
90–105	32–41	Moderate	Extreme Caution	Heat cramps, heat exhaustion, and heat stroke possible with prolonged exposure and/or physical activity
105–130	41–54	High	Danger	Heat cramps and heat exhaustion are likely. Heat stroke probable with prolonged exposure and/or physical activity
> = 130	> = 54	Very high to extreme	Extreme danger	Heat stroke is highly likely and imminent

$$HI = -42.379 + 2.04901523*T + 10.14333127*RH - 0.2247554*T*RH - 6.8378*10^{-3}*T^2 - 5.48172*10^{-2}*RH^2 + 1.229*10^{-3}*T^2*RH + 8.528*10^{-4}*T*RH^2 - 1.99*10^{-6}*T^2*RH^2 \quad (1)$$

where T is temperature in degrees Fahrenheit (°F) and RH is relative humidity in percent. This formulation was developed through a multiple regression analysis of the Steadman (1979) equation for apparent temperature (which takes into account many physiological and environmental factors) in order to adopt two commonly used and conventional variables (i.e., ambient air temperature and relative humidity). HI is thus the heat index expressed as an apparent temperature in degrees Fahrenheit.

This full regression equation is only appropriate when the values of temperature and humidity generate *HI* greater than 80 °F (i.e., 27 °C). In this case, a number of adjustments are applied to this formula depending on the values of temperature and relative humidity.

First, if *RH* is less than 13% and *T* is between 80 °F and 112 °F, the following adjustment is subtracted from *HI:*

$$Adjustment1 : \left(\frac{13 - RH}{4}\right) * \sqrt{\left(17 - \frac{|T - 95|}{17}\right)} \quad (2)$$

Second, if *RH* is greater than 85% and *T* is between 80 °F and 87 °F, the following adjustment is added to *HI*:

$$Adjustment2 : \left(\frac{RH - 85}{10}\right) * \left(\frac{87 - T}{5}\right) \quad (3)$$

The Rothfusz (1990) formulation (i.e., equation (1)) along with the adjustments is not appropriate when conditions of temperature and humidity result in a *HI* value lower than 80 °F (i.e., 27 °C). In this case, the following formula is applied:

$$HI = 0.5*[T + 61 + (T - 68)*1.2 + RH*0.094] \quad (4)$$

The *HI* values are calculated for each day and then used to compute seasonal averages. The seasonal values are sorted by ranges, and a category defining the level of heat stress is assigned to each range. Table 1 summarizes the different HI ranges, the corresponding levels of heat stress (i.e., categories), and the health problems that can result from each level. The categories are classified from Safe and Caution to Extreme Danger (i.e., Table 1), with possible health-related problems such as fatigue, heat cramps, heat exhaustion, and/or heat stroke that can occur with prolonged exposure and/or physical activity. The *HI* values described above are valid for shady locations only with light wind conditions. Exposure to sunshine and strong winds, which often occur in West Africa, can increase heat stress. Therefore, the *HI* values provided here can be considered as representing minimal effects and risk levels for the conditions of West Africa.

It should be noted that the HI index used here and the related risk levels do not take into account heat wave and are rather used for heat stress assessment. It has been used worldwide in a number of studies, as it shows the highest consistency with the original equation of apparent temperature (Anderson et al., 2013). These

Table 2
Summary of Discomfort Index (DI) Ranges Along With Portion of the Population It Affects

DI (°C)	Population at risk
= < 21	No significant heat discomfort: Safe
21–24	Less than 50% of the population is in discomfort
24–27	More than 50% of the population is in discomfort
27–29	Most of the population is in discomfort
29–32	Severe stress: everyone feels stress
> = 32	State of medical emergency

studies include Diffenbaugh et al. (2007) focusing on the Mediterranean region; Oleson et al. (2015) applying it for United States and Canada; Lee and Brenner (2015) employing it for the entire globe; and Ropo et al. (2017) focusing over London and South Africa.

To provide an indicator of threat to the population well-being, a simplified human discomfort index (hereafter referred as DI) is devised following the formulation of Thom (1959) and Sohar et al. (1963):

$$DI = 0.5{*}T_C + 0.5{*}T_W \tag{5}$$

where DI is the discomfort index (unitless), T_C is the actual temperature in degrees Celsius, and T_W is the wet bulb temperature in degrees Celsius. Also, in this case DI values are first calculated for each day and then used to compute seasonal averages. Seasonal values are categorized into different classes providing information on the proportion of human population at risk (see Table 2). As a simplified index, the percentage attached to each range of DI should not be considered as quantitatively robust but rather as a general indicator of increasing proportions of population feeling heat discomfort as the index value increases. This index has also been applied in various regional climatic contexts, including Europe and the Mediterranean area (i.e., Bartzokas et al., 2013; Giles et al., 1990; Poupkou et al., 2011), the Middle East (Epstein & Moran, 2006; Ghani et al., 2017), and Africa (Bady, 2014; Yousif & Tahir, 2013).

For the purpose of HI validation, we use temperature and relative humidity fields from the National Center for Environmental Predictions (NCEP 2.5° × 2.5° resolution; Kalnay et al., 1996) and the European Re-Analysis Interim (ERA-Interim 1.5° × 1.5° resolution; Dee et al., 2011). To account for uncertainties in these parameters (i.e., Diallo et al., 2012), temperature observations from the University of Delaware (UDEL v4.01; 0.5° × 0.5° resolution; Lawrimore et al., 2011) and the Climatic Research Unit of the University of East Anglia (CRU v4.01; 0.5° × 0.5° resolution; Harris et al., 2014) data sets are also combined with relative humidity from NCEP and ERA-Interim. However, results based on these latter data sets are shown as supporting information (i.e., Figures S1 and S2).

NCEP, ERA-Interim, and the combinations UDEL/NCEP and UDEL/ERA-Interim as well as CRU/NCEP and CRU/ERA-Interim are used to assess the CORDEX experiments during the reference period, which is here taken as 1979 through 2005 in the observation and reanalysis data sets (common to NCEP, ERA-Interim, UDEL, and CRU) and the 30-year period when the driving GCM simulates a 0.48 °C increase of global mean temperature compared to the preindustrial period in the model simulations (see supporting information).

Projected changes are calculated as Future (1.5 °C or 2 °C scenarios of global warming) minus Reference. Changes in the area extent of each of the different HI and DI categories are expressed as percent of the total area extent of our domain of interest (i.e., Figure 1). Similarly, changes in the frequency of each HI and DI category are expressed as percent of the length of the year (i.e., 365 days).

3. Results

3.1. Validation

Heat stress classifications applied to the NCEP, ERA-Interim, and CORDEX ensemble during the reference period are intercompared for each season (i.e., December–January [DJF], March–May [MAM], June–August [JJA], and September–November [SON]) in Figure 2. Results based on UDEL/NCEP, UDEL/ERA-Interim, CRU/NCEP, and CRU/ERA-Interim are reported in Figures S1 and S2. For present-day climate, NCEP and ERA-Interim show that most of West Africa is in safe conditions except along the Gulf of Guinea (i.e., from Cote d'Ivoire to Nigeria), where the Caution category prevails. The areas with Caution extend further north in MAM to reach the southern Sahel and northern Sahara regions covering most of Mauritania, Mali, Niger, and Chad. Similar conditions are found in the UDEL/NCEP, UDEL/ERA-Interim, CRU/NCEP, and CRU/ERA-Interim data sets. During the same season, Extreme Caution conditions emerge in some portions of the countries throughout the Gulf of Guinea, for example, Cote d'Ivoire, Ghana, and Nigeria, and also further north over the Sahel in Burkina Faso and Chad. These conditions are more prominent in ERA-Interim. Substantial discrepancies exist between NCEP and ERA-Interim over these regions, where the latter produces Extreme Caution conditions along the whole northern Gulf of Guinea and southern Sahel. These conditions are more extended in

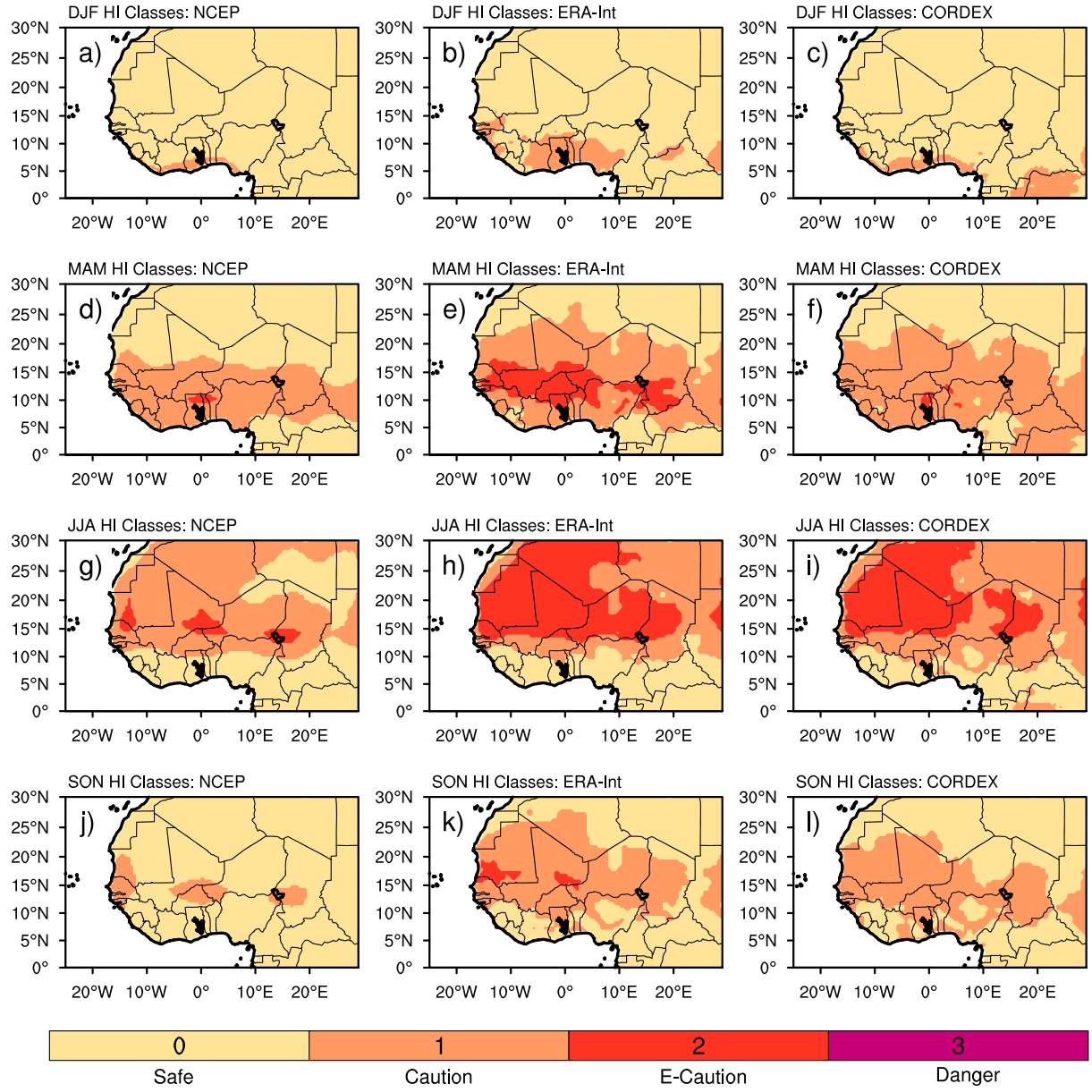

Figure 2. Distribution of seasonal heat stress categories in the reference period for NCEP (a, d, g, and j), ERA-Interim (b, e, h, and k), and CORDEX multimodel ensemble mean (c, f, i, and l). In the figure, HI stands for heat index and E-Caution is for Extreme Caution. NCEP = National Center for Environmental Predictions; CORDEX = COordinated Regional climate Downscaling EXperiment; JJA = June–August; MAM = May–May; DJF = December–February; SON = September–November.

UDEL/NCEP, UDEL/ERA-Interim, CRU/NCEP, and CRU/ERA-Interim compared to NCEP but less extensive compared to ERA-Interim. In JJA, the Sahel countries (i.e., from Senegal to Chad) and the western Sahara regions (i.e., Mauritania and Algeria) are subject to heat stress with moderate risk levels.

Prominent differences between the NCEP and ERA-Interim combinations appear, with the former showing only few areas with the Extreme Caution category. This raises the issue of uncertainties in the temperature and relative humidity data and the subsequent heat indices observed over these areas. However, it is worth noting that UDEL/NCEP, UDEL/ERA-Interim, CRU/NCEP, and CRU/ERA-Interim are more consistent to ERA-Interim than to NCEP, indicating that the NCEP temperature values may be underestimated. In the Gulf of Guinea and orographic regions, Safe conditions predominate in response to low temperatures offsetting the high relative humidity. SON is characterized by a low level of risk (Caution class) in the Sahel countries

and portions of the Gulf of Guinea, with Safe conditions around orographic regions (due to low temperatures) and desert areas (due to low relative humidity). This is shown in the ERA-Interim, UDEL/NCEP, UDEL/ERA-Interim, CRU/NCEP, and CRU/ERA-Interim data sets, while NCEP underestimates the risk levels.

The multimodel ensemble of CORDEX RCMs provides similar patterns of heat stress classification across the different seasons with respect to ERA-Interim and the majority of the different data set combinations. In particular, the ensemble captures the emerging Caution level in DJF over the Gulf of Guinea, although this is more confined along the coastlines. In addition, a hint toward the presence of Extreme Caution areas in some countries over the Gulf of Guinea and the Sahel during MAM is reproduced but with a lower spatial extent (more similar to NCEP). Furthermore, in JJA the multimodel ensemble simulates a northward migration and extension of the Extreme Caution category within the range of the differences found between the NCEP, ERA-Interim, and other combinations of data sets. Finally, the prevalence of Safe and Caution conditions shows a distribution in good agreement with observations.

We also assess the interannual variability of HI using as a metric the coefficient of variation (hereafter referred as CV), calculated as the standard deviation divided by the mean (i.e., Figure 3) and expressed as a percentage value. The use of the CV has the advantage of removing the dependence of the standard deviation on the mean (Giorgi & Bi, 2005). The CV is computed for each RCM experiment, and it is then averaged across the RCMs to obtain the multimodel ensemble mean. The largest interannual variability values shift from one region to another depending on the season. In DJF, the highest variability from NCEP and ERA-Interim is observed in the Sahara, while the lowest values are found in the Gulf of Guinea. In MAM, Caution and Extreme Caution conditions in the Sahel are more persistent throughout the year, while in JJA, both Caution and Extreme Caution conditions in the Sahel are subject to pronounced variability that can lead to higher risk levels. In SON, the largest variability occurs in the Sahel and the Sahara desert, while the Gulf of Guinea experiences more persistent HI conditions. The multimodel ensemble mean reproduces reasonably well the observed spatial distribution of the CV, providing values that are within the range of the NCEP and ERA-Interim reanalysis, although with a slight underestimation in SON over some portions of Nigeria. In summary, considering both the climatology and the interannual variability of HI, it is assessed that the performance of the CORDEX multimodel ensemble mean in simulating mean and variability of this index, along with the resulting heat stress classes, is acceptable.

In general, it is evident from the climatology that during the reference period West Africa does not experience significant dangerous and/or extremely dangerous heat stress (i.e., Danger and/or Extreme Danger classes). The highest risk level occurring in the reference period over the region is Extreme Caution in MAM and JJA with a CV lying between 4% and 6% of the mean. How these categories shift, extend, and possibly intensify in future climate conditions under the 1.5 °C and 2 °C global warming scenarios is examined in the next section.

3.2. Projected Changes in Heat Stress and Human Discomfort Classification

Projected changes (1.5 °C or 2 °C minus reference) indicate a general increase of HI and DI values across the whole region and all seasons (see also Figures S3 and S4). Such increases are statistically significant at the 95% confidence level. While for DI the largest changes occur in the Sahara desert and the Sahel for all seasons, in the case of HI, they are located over the Sahara in DJF, the Gulf of Guinea in MAM, and along the southern Gulf of Guinea and the Sahel in JJA and SON. The differences between the changes in the 1.5 °C and 2 °C warming scenarios range between 6% and 10% and are statistically significant at the 95% confidence level. This implies that heat stress risk levels may be higher and/or will be more spatially extended compared to the reference period and that reducing the global warming by 0.5 °C can decrease the stress risk by as much as 10%.

To further investigate this issue, seasonal heat stress values for the reference period and the 1.5 °C and 2 °C global warming scenarios are shown in Figure 4. In DJF, compared to the reference period, the multimodel ensemble projects for both scenarios a small extension of the Caution areas further in the northern Gulf of Guinea and along the coastlines reaching southern Senegal. The areas with moderate risk level for the Extreme Caution category considerably broaden in MAM to cover the whole Gulf of Guinea and most of the Sahel countries but not reaching the orographic zones of the Guinea highlands, Cameroon Mountains, and Joss Plateau (probably because of small temperature and humidity changes). In these latter zones,

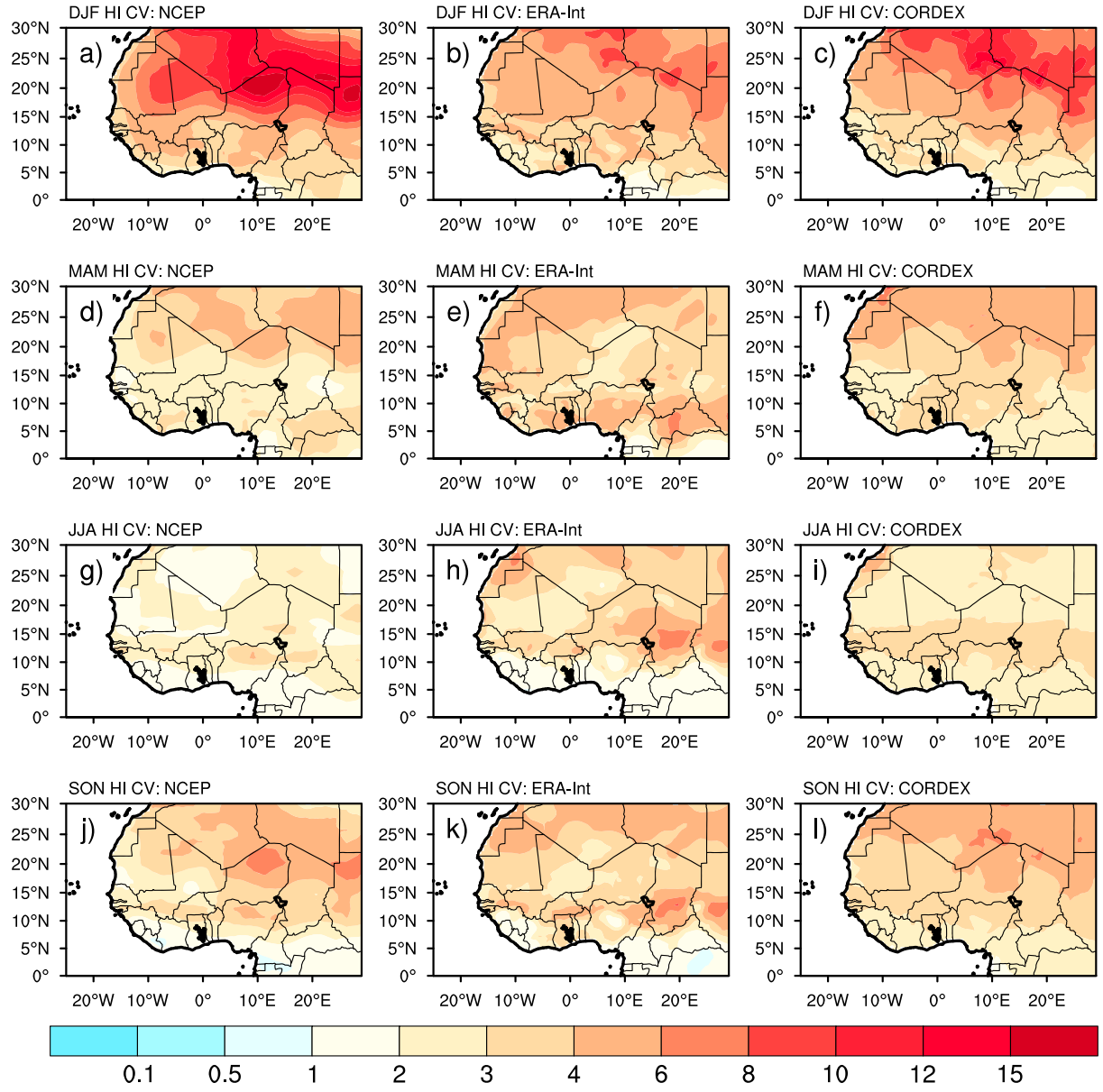

Figure 3. Distribution of seasonal coefficient of variation (i.e., CV) of the HI in the reference period for NCEP (a, d, g, and j), ERA-Interim (b, e, h, and k), and CORDEX multimodel ensemble mean (c, f, i, and l). In the figure, HI stands for heat index and E-Caution is for Extreme Caution. Units are in percent of the corresponding mean values. NCEP = National Center for Environmental Predictions; CORDEX = COordinated Regional climate Downscaling EXperiment; JJA = June–August; MAM = May–May; DJF = December–February; SON = September–November.

Caution conditions prevail. In JJA, the multimodel ensemble projects a recession of Safe conditions, which are now confined around orographic regions, a southward shift of the areas with the Caution category covering the whole Gulf of Guinea and more extensive zones with Extreme Caution encompassing most of the Sahel and the Sahara desert. In SON, Caution conditions are more common for both scenarios but a small area of Extreme Caution level emerges in Senegal and extends eastward.

In general, across the different seasons (except in DJF), the extension of areas in the Extreme Caution class is greater in the 2 °C than in the 1.5 °C global warming scenario. This implies that heat cramps, heat exhaustion, and heat stroke can occur with prolonged exposure and/or physical activity in both scenarios but with the 2 °C scenario having a larger influence. These risks become more common in the Sahel (i.e., Senegal, Mali, Burkina Faso, Niger, and Chad) and the Gulf of Guinea (i.e., Cote d'Ivoire, Ghana, Nigeria) during MAM, over

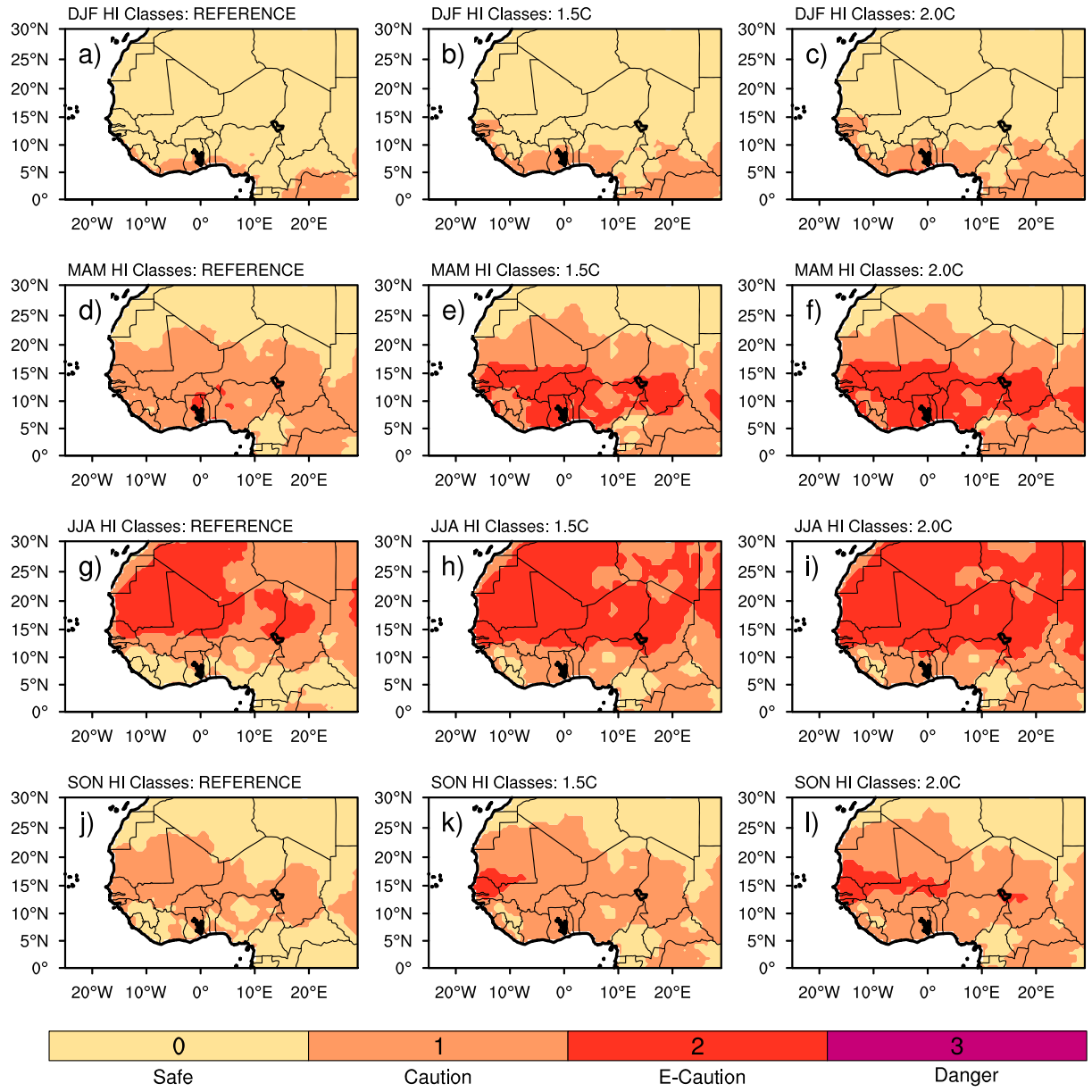

Figure 4. Distribution of seasonal heat stress categories from CORDEX multimodel ensemble mean for the reference period (a, d, g, and j), for the 1.5 °C global warming scenario (b, e, h, and k), and for the 2 °C global warming scenario (c, f, i, and l). In the figure, HI stands for heat index and E-Caution is for Extreme Caution. CORDEX = COordinated Regional climate Downscaling EXperiment; JJA = June–August; MAM = May–May; DJF = December–February; SON = September–November.

most of the Sahel (i.e., Senegal, Mali, Burkina Faso, Niger, and Chad) and the Sahara desert (Mauritania, Algeria, and Libya) during JJA, and over Senegal, central Mali, and southern Niger in SON. It is thus evident that countries such as Senegal, Mali, Niger, and to a lesser extent Burkina Faso and Chad are more exposed to increased heat-related occupational health and safety risks.

Although the analysis above indicates an increased risk toward the occurrence of more heat-related illness, it does not provide insights about the proportion of the population at risk. Figure 5 presents the reference and projected human DI under both global warming targets. During the reference period and across the seasons, Safe HI conditions overlap with areas with no heat discomfort. Similarly, the Caution category mostly overlaps with regions where less than 50% (L50) of the population is in discomfort. The Extreme Caution heat class mostly overlaps with regions where more than 50% (M50) of the population experiences heat discomfort, where however the M50 regions are more spatially extended. For example, in MAM they concern

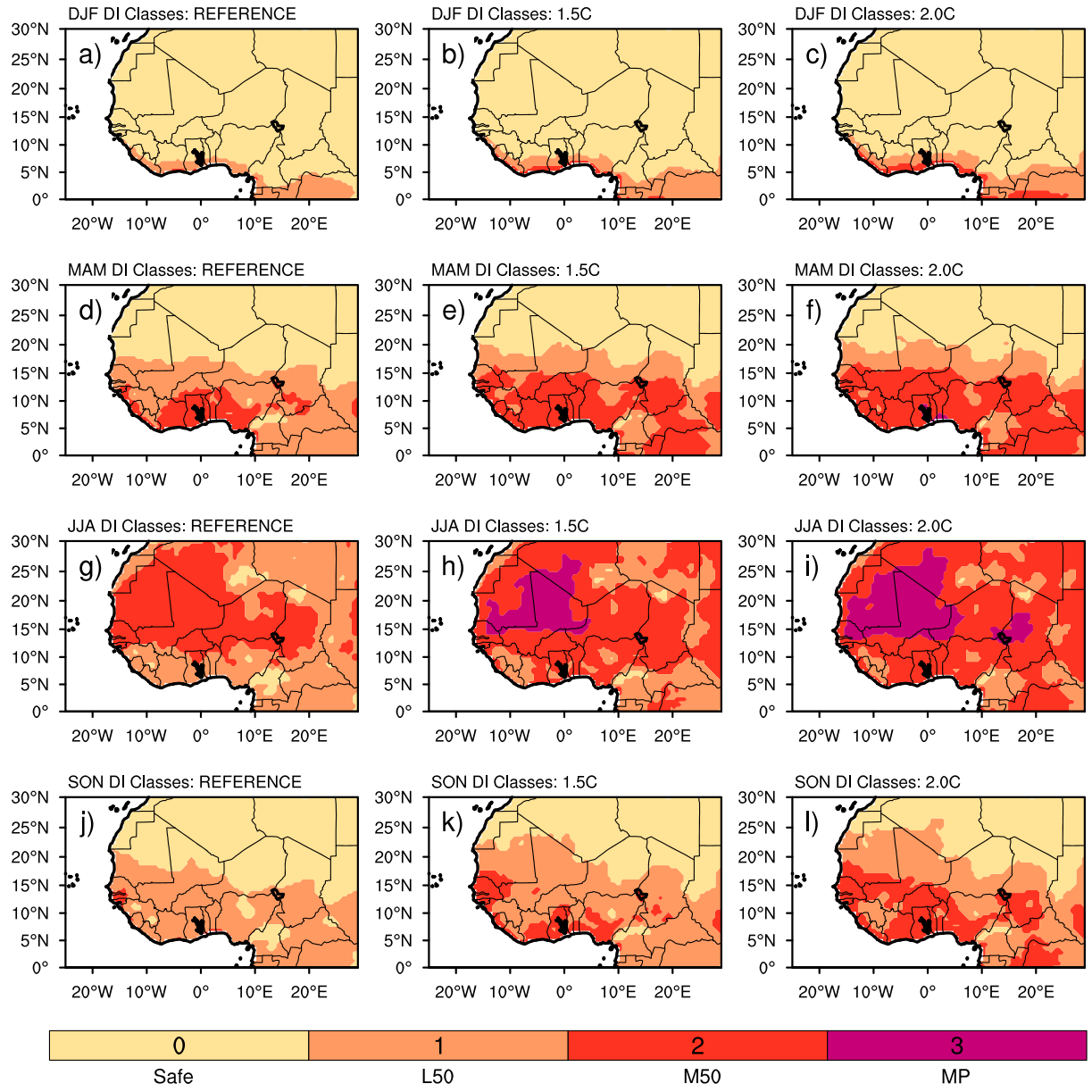

Figure 5. Distribution of seasonal discomfort categories from CORDEX multimodel ensemble mean for the reference period (a, d, g, and j), for the 1.5 °C global warming scenario (b, e, h, and k), and for the 2 °C global warming scenario (c, f, i, and l). In the figure, DI stands for discomfort index, L50 is *less than 50% of population is at discomfort*, M50 is *more than 50% of population is at discomfort*, and MP is *most of the population is at discomfort*. CORDEX = COordinated Regional climate Downscaling EXperiment; JJA = June–August; MAM = May–May; DJF = December–February; SON = September–November.

populations from the Gulf of Guinea to the southern Sahel as well as the coastlines of the Guinea highlands, thus hitting countries such as Sierra Leone, Cote d'Ivoire, Ghana, Nigeria, and Burkina Faso. In JJA these conditions are more limited to countries along the Sahel band and western Sahara including Senegal, Mauritania, Mali, and Niger. Both in the 1.5 °C and 2 °C global warming scenarios population at risk increases along the coastlines of the Gulf of Guinea in DJF, where more than 50% of local population is projected to experience heat discomfort. During MAM, this M50 is widespread over the Gulf of Guinea and southern Sahel states as a result of the occurrences of heat stress classified as Extreme Caution. In JJA, two DI classes are prominent. In northern Sahel and western Sahara, for both scenarios, the proportion of population at risk increases from more than 50% to almost everyone (most of the population is at discomfort), implying that most people in these regions are vulnerable to heat-related pathologies during strenuous activity or prolonged exposure.

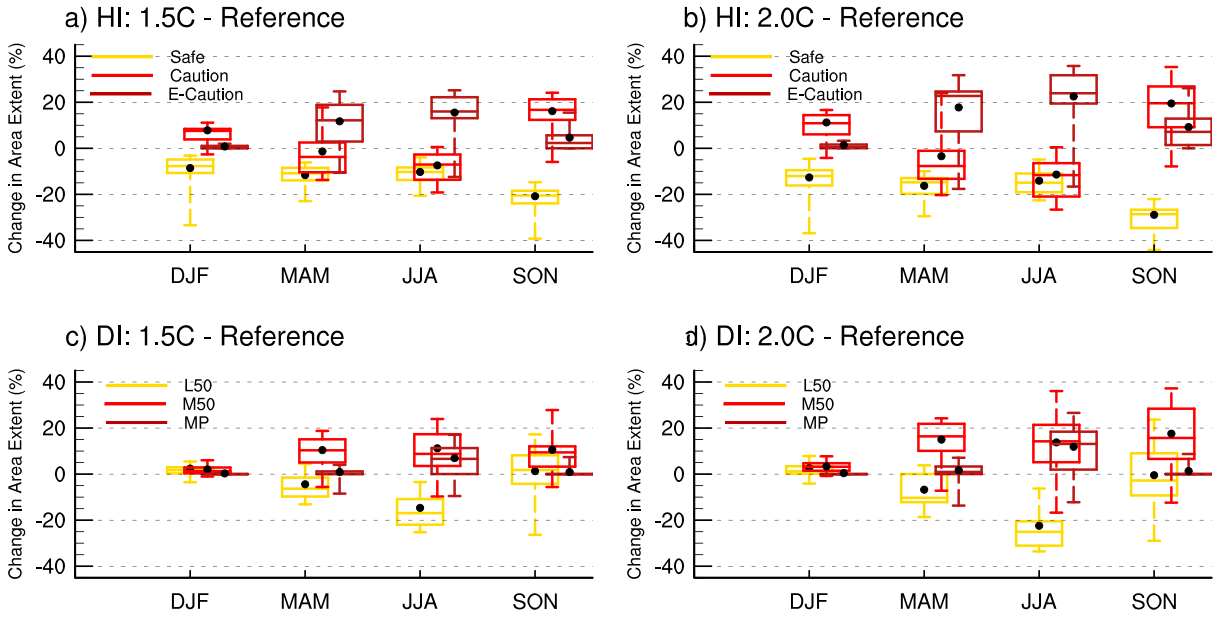

Figure 6. Change (global warming scenario minus reference period) in the fractional area extent occupied by each of the heat stress (a, b) and discomfort (c, d) categories for the 1.5 °C (a, c) and 2 °C (b, d) global warming scenarios from CORDEX multimodel ensemble means. Changes are expressed as percent of total area extent (i.e., Figure 1). In the figure, HI stands for heat index, DI stands for discomfort index, E-Caution is *Extreme Caution*, L50 is *less than 50% of population is at discomfort*, M50 is *more than 50% of population is at discomfort*, and MP is *most of the population is at discomfort*. The black dots denote the multimodel ensemble means, and the different percentiles depicted in each box-and-whisker are, respectively, the ensemble 95th, 75th, 50th (i.e., the median), 25th, and 5th percentiles. CORDEX = COordinated Regional climate Downscaling EXperiment; JJA = June–August; MAM = May–May; DJF = December–February; SON = September–November.

In all other regions of West Africa except over orographic zones, the projections indicate that these heat stress-related illnesses threaten more than 50% of population. Similar conditions are projected in the Sahel (i.e., Senegal) and the Gulf of Guinea (Cote d'Ivoire, Ghana, and Nigeria) during SON.

In general, while both scenarios indicate increased levels of threat to local population compared to the reference period, the areal coverage is wider in the 2 °C global warming scenario. For instance, in JJA, areas where most populations are at risk extend to Senegal and Chad and include wider regions in Niger and Mauritania in the 2 °C compared to the 1.5 °C global warming scenario. Also in MAM and SON, the zones at risk for more than 50% of the population stretch northward and eastward in the Sahel.

Supporting Information Figures S7–S10 show the 25th and 75th percentiles of the model ensemble for both the HI and DI classes. They show categories of heat stress and discomfort level that are in line with the ensemble mean. As can be seen, the categories are the same in the ensemble mean and interquartile range, although the area extents of the higher risk levels are substantially larger in the 75th percentile than in the 25th percentile and the ensemble mean. This indicates that the projected heat stress and related risk levels as well as proportion of human population in heat discomfort are consistent among the RCM experiments and that the uncertainty is only related to their areal coverage.

For a more quantitative assessment of the projected areal extents of heat stress conditions, and of the uncertainty across the different RCMs, Figure 6 shows the seasonal mean changes and intermodel spread for each HI and DI class as box-and-whisker plots for the different global warming scenarios. In the 1.5 °C scenario, the most prominent feature is a reduction in area extent of heat indices that warrant Safe conditions, with the largest changes (−20% compared to the total area of the domain of interest) occurring in SON. Also the area extent of the Caution category is projected to decrease, especially in MAM and SON, at the expenses of a limited increase (~7% of total area) in areal coverage of the heat stress class Caution in DJF, a relatively substantial extension of areas with heat stress risk level Extreme Caution in MAM (~12% of total area) and in JJA (~15% of total area) and a stretching of both Caution (17% of total area) and Extreme Caution (5% of total area) category zones in SON. The 2 °C global warming scenario shows similar features, but the changes are substantially larger. For example, the decreased areal coverage of Safe conditions is about 27% in SON while the areal extension of Extreme Caution level in MAM, JJA, and SON reaches, 20%, 25%, and 10% of the total area, respectively.

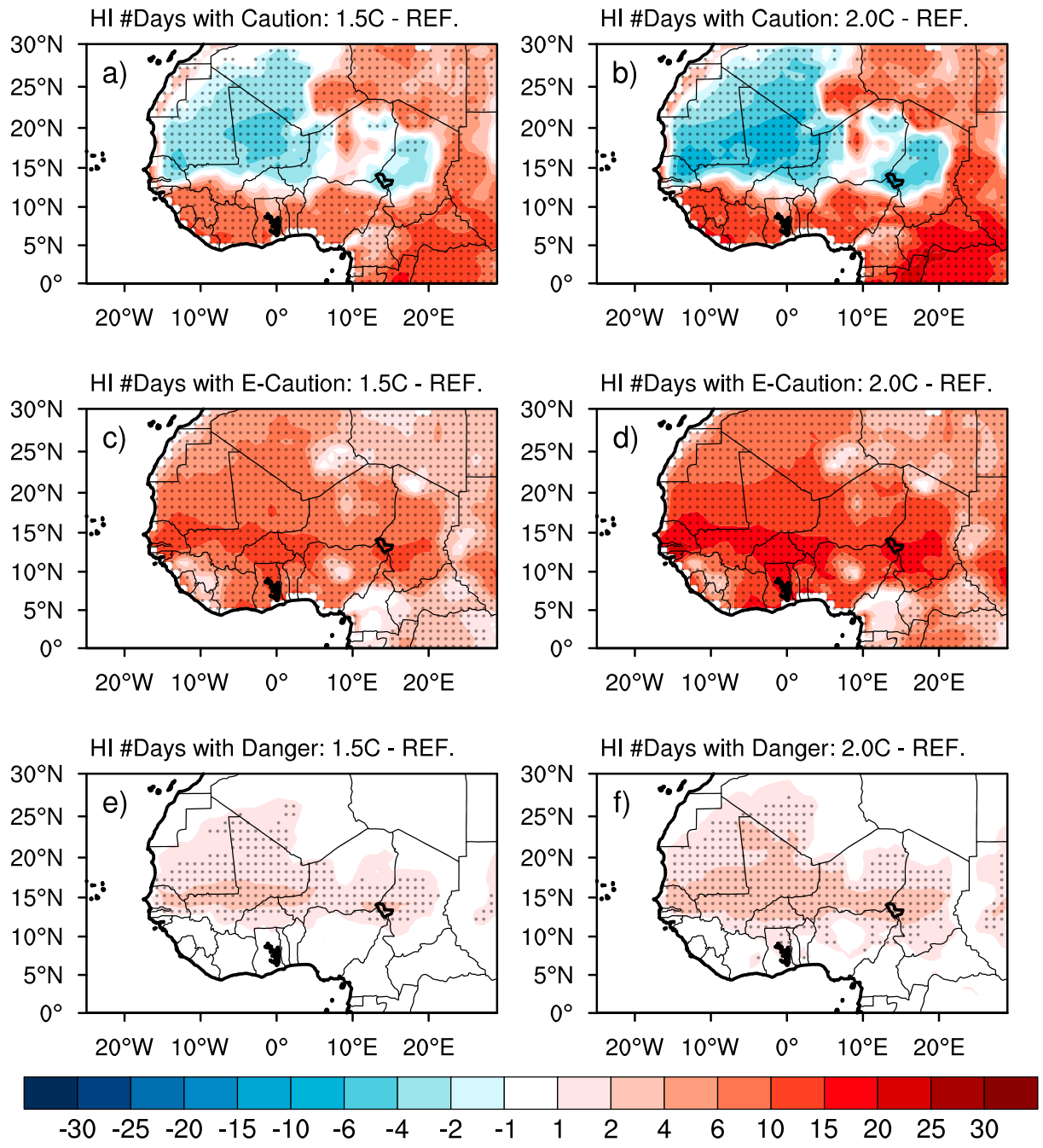

Figure 7. Change (global warming scenario minus reference period) in the frequency of each of the heat stress category for the 1.5 °C (a, c, and e) and 2 °C (b, d, and f) global warming scenarios from CORDEX multimodel ensemble means. Changes are expressed as a percent of the length of the year (i.e., 365 days). Dotted areas are where 75% of the RCMs agree in the sign of the changes. In the figure, HI stands for heat index and E-Caution is for Extreme Caution. CORDEX = COordinated Regional climate Downscaling EXperiment; RCMs = regional climate models; JJA = June–August; MAM = May–May; DJF = December–February; SON = September–November.

Concerning the DI, in both scenarios no noticeable changes occur in DJF, while an extension of areal coverage for regions where more than 50% of the population is in discomfort is projected in MAM, JJA, and SON. The changes are about 10% for 1.5 °C and 15% to 19% of the total area for the 2 °C. The area extent where less than 50% of population is at risk shows no changes (i.e., in DJF and SON) or some slight decreases (i.e., MAM and JJA). It is noted that, consistent to Figure 4, the extension of regions where more than 50% of population is in discomfort closely follows that of the Extreme Caution category of heat stress. Another notable feature is the appearance of zones in JJA where most of the population feels

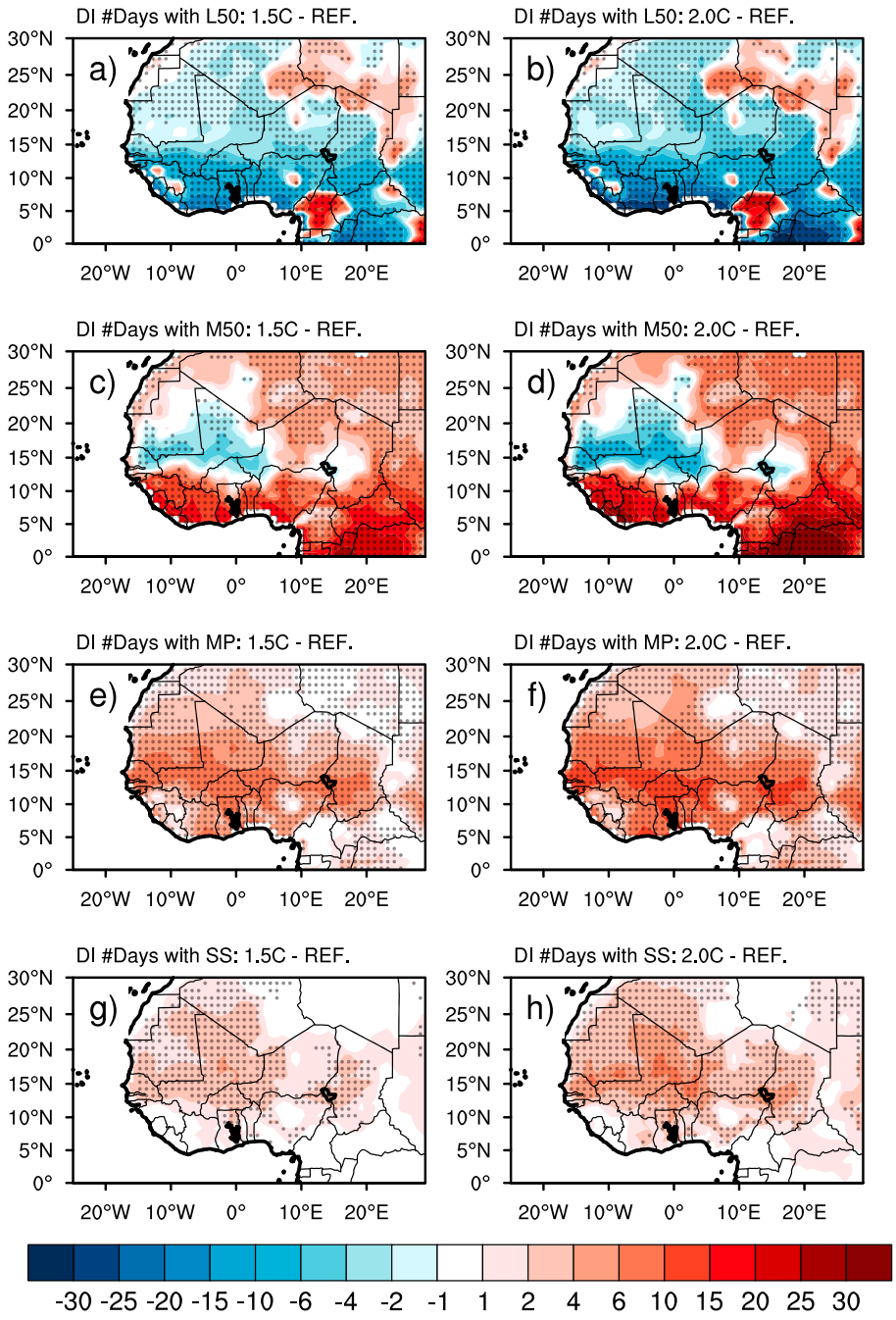

Figure 8. Change (global warming scenario minus reference period) in the frequency of each of the discomfort category for the 1.5 °C (a, c, e, and g) and 2 °C (b, d, f, and h) global warming scenarios from CORDEX multimodel ensemble mean. Changes are expressed as a percent of the length of the year (i.e., 365 days). Dotted areas are where 75% of the RCMs agree in the sign of the changes. In the figure, DI stands for discomfort index, L50 is *less than 50% of population is at discomfort*, M50 is *more than 50% of population is at discomfort*, MP is *most of the population is at discomfort*, and SS is *Severe State where everyone is at discomfort*. CORDEX = COordinated Regional climate Downscaling EXperiment; RCMs = regional climate models.

discomfort that was not present during the reference period. These regions cover about 7% and 12% of total area, respectively, for the 1.5 °C and 2 °C scenarios of global warming. Therefore, global warming, even when limited to 1.5 °C, puts a higher proportion of human population at risk of heat-related occupational illnesses and injuries over West Africa.

The uncertainty analysis reveals similar characteristics for the HI and DI indices. The interquartile ranges are larger in MAM and JJA and in the 2 °C compared to the 1.5 °C scenario. This suggests that, as temperature increases seasonally (in MAM and JJA compared to DJF and SON) and global warming intensifies (from 1.5 °C to 2 °C), the range of regional responses of the individual CORDEX models tends to increase. However, it is noted that the sign of the ensemble median as well as that of the lower (25th percentile) and upper (75th percentile) quartiles mostly follows the mean changes, implying robustness in the results.

It should be emphasized that, although some heat stress (Danger and Extreme Danger) and discomfort (Severe stress and State of medical emergency) classes do not appear in the climatology of the indices, it is not excluded that they might occur on individual days, both in the reference period and in the scenarios. The frequencies of days in different categories are thus analyzed in the following section.

3.3. Projected Changes in the Frequency of Heat Stress Categories and Population at Risk

Changes in the frequency of each of the heat stress categories in both 1.5 °C and 2 °C global warming scenarios are shown in Figure 7. The frequency of days in the Caution category is projected to decrease by about 4% to 10% (of the length of the year) in Western Sahara and northern Sahel and to increase by about 6% to 15% in the southern Sahel and the Gulf of Guinea, with the 2 °C scenario providing the largest changes. The number of days with a heat stress level of Extreme Caution generally increases throughout West Africa, with the most substantial changes (up to 15% and 20% in the 1.5 °C and 2 °scenarios respectively) along the Sahel and few regions in the Gulf of Guinea. These more frequent and severe heat stress conditions affect thus countries such as Senegal, Mali, Burkina Faso, and few regions in southern Niger, northern Ghana, southern Cote d'Ivoire, and western Nigeria. Of particular interest is the occurrence and lengthening (up to 2% to 4% of the length of the year) of the severe heat stress of category Danger over most of the Sahel and the Sahara desert. Although both scenarios project similar magnitudes for this high risk level, the largest changes are more spatially extended in the 2 °C scenario impacting countries such as Senegal, Mali, Burkina, Niger, and Chad.

The projected changes for discomfort level and proportion of affected population are presented in Figure 8. The occurrence of days with less than 50% of the population in discomfort generally decreases throughout West Africa (except over the mountain peaks). The largest decreases of about 20% to 25% are projected in the Gulf of Guinea and in the 2 °C scenario. Consistently, with this decrease in comfort conditions, an increased frequency of days with more than 50% of the population at risk is projected over the same regions. In general, global warming produces more days in which most of the populations are in discomfort across West Africa. These days become more frequent along the Sahel band and portions of the Gulf of Guinea, where increases in their frequency range from 10% to 15% of the length of the year. These changes are associated with more occurrences of the Extreme Caution heat stress category.

Finally, days with severe stress during which everyone feels heat discomfort emerge and become more prevalent in almost all West Africa, except around orographic regions. While in the 1.5 °C global warming scenario the largest increases are limited to 4%, in the 2 °C scenario they reach 6% to 10% of the length of the year and affect countries such as Senegal, Mali, Burkina Faso, Niger, and Chad. This means that an increase of up to 36 (15) days during which the entire population feels heat discomfort is projected under the 2 °C (1.5 °C) global warming scenario.

4. Conclusion and Discussion

Climate change is considered as one of the main challenges for environmental and developmental issues in Africa, putting directly human health and productivity at risk through occupational heat stress. Over West Africa, information is lacking on the extent of future heat stress and its consequences, especially in occupational settings. In this study, we employ a heat index combined with a simplified human DI to assess projected changes in heat stress severity and spatial extension along with the proportion of population that is at risk. In line with the Paris Agreement, we consider two global warming scenarios: 1.5 °C and 2 °C global temperature increase compared to the preindustrial period, where these scenarios are extracted from an ensemble of CORDEX-Africa RCM projections.

The results first show that the multimodel ensemble of CORDEX RCMs reproduces reasonably well the occurrence and spatial extent of the different heat stress categories across the different seasons. Few discrepancies

exist between the combinations of observed temperature and humidity data sets used to validate the simulations, and the CORDEX ensemble provides values mostly within the range of these data sets.

Projected heat stress classifications under the 2 °C warming scenario compared to the reference period show that while the Caution category still prevails in DJF, the Extreme Caution class substantially extends to cover the Gulf of Guinea and the Sahel in MAM (up to 20% of total area), the Sahel and Sahara desert in JJA (up to 25% of total area), and only the Sahel band in SON (up to 10% of total area). These expansions occur at the expenses of the Caution and Safe categories that decrease by up to 10% to 27% of the total domain area. In the 1.5 °C global warming scenario these area extents are limited to 12%, 15%, and 5% of total domain area.

Similarly, projected human discomfort measured by the proportion of population at risk shifts from less than 50% to more than 50% over most of West Africa, in line with the Extreme Caution heat stress category. These changes in the area extent range from 15% to 19% (for different seasons) for the 2 °C scenario versus 10% to 12% for the 1.5 °C scenario. It is noted that a high risk level of human discomfort (i.e., most of the population feels heat discomfort) that did not exist in the reference period emerges in the Sahel and the western Sahara in both global warming scenarios. Therefore, due to the extension of the heat stress category Extreme Caution, most of the population in the region is expected to become vulnerable to possible heat cramp, exhaustion, and/or heat stroke during physical activity or prolonged exposure. It should be emphasized that for both indices, the sign of the median, upper, and lower quartiles closely follows that of the corresponding mean changes. This suggests that most of the RCMs agree in the direction of changes of spatial extent for the different heat stress and human discomfort categories, thus implying more robust results. Changes in areal extent are generally larger in the 2 °C than in the 1.5 °C scenario and are largely due to a substantial increase of temperature combined with a slight decrease of relative humidity.

Changes in the frequency (i.e., number of days) of each of the different heat stress categories are also analyzed. Of notable interest is the increased frequency (up to 20% of the length of the year) in the occurrences of Extreme Caution category in almost all West Africa and the appearance and increasing number (up to 2% to 4% of the length of the year) of days with the more severe heat stress of category Danger affecting mostly the Sahel and the Sahara desert. Consistent with these changes, the number of days with more than 50% of population at risk substantially increases in the Gulf of Guinea and decreases in the Sahel and western Sahara. It is shown that such changes are consequences of more frequent and recurrent occurrences of days (up to 10% of the length of the year) where most of population or everyone is at risk. These conditions concern countries such Senegal, Mauritania, Mali, Burkina Faso, Niger, and Chad and are generally more frequent in the 2 °C than in the 1.5 °C scenario.

From these results it is evident that population in West Africa will face unprecedented heat discomfort even in the case of the Paris global warming scenario targets. This discomfort would of course be much more severe and extended if these targets were to be exceeded. Exposure to direct sunlight and stronger winds can increase the level of risk (Rothfusz, 1990; Steadman, 1979), indicating that the most vulnerable people to heat-related illnesses are workers who spend a substantial portion of the shift outdoors and those who work in hot and humid environment indoors. They include agricultural workers, miners, fishermen, construction/building workers, electricians, landscapers, ground maintenance, and factory workers (Bourbonnais et al., 2013; Lucas et al., 2014). Considering the agriculture sector as an example, it employs 60% of the active labor force and accounts for 35% of the gross domestic product in West Africa (Mensah et al., 2016). Therefore, the projected heat stress threatening the workers health can reduce productivity and undermine the region's economic development.

It should be noted that not everyone reacts to the heat stress in the same way. The response differs from person to person depending on medical condition, level of fitness, body weight, age, and economic situation (National Institute for Occupational Safety and Health, 2016). In any case, protective measures need to be implemented to mitigate and to adapt to the projected heat stress, even under the Paris scenario targets. These can be either engineering and/or work practice controls designed to decrease heat stress. Engineering control measures consist of implementing cooling systems, air conditioning, using reflective or heat-absorbing shielding or barriers and reducing steam leaks, wetness, and humidity. Work practice control measures include acclimatization, hydration, and decrease of metabolic demands of activities through regular and longer breaks or rescheduling of activities to cooler period of the day.

Acknowledgments
This work is fully supported by the German Federal Ministry of Education and Research through the West African Science Service Center on Climate Change and Adapted Land Use (WASCAL). The data sets used in this study are directly downloaded and available from the Earth System Grid Federation (ESGF), specifically the DKRZ (https://esgf-data.dkrz.de/projects/esgf-dkrz/) and the SMHI nodes (https://esg-dn1.nsc.liu.se/projects/esgf-liu/). Therefore, the authors would like to acknowledge CMIP5 and CORDEX modeling centers as well as the ESGF. The authors declare no competing interests.

References

Akinsanola, A. A., Ajayi, V. O., Adejare, A. T., Adeyeri, O. E., Gbode, I. E., Ogunjobi, K. O., et al. (2017). Evaluation of rainfall simulations over West Africa in dynamically downscaled CMIP5 global circulation models. *Theoretical and Applied Climatology*, *132*, 437–450. https://doi.org/10.1007/s00704-017-2087-8

Anderson, G. B., Bell, M. L., & Peng, R. D. (2013). Methods to calculate the heat index as an exposure metric in environmental health research. *Environmental Health Perspectives*, *121*(10), 1111–1119. http://doi.org/10.1289/ehp.1206273

Anderson, G. B., Oleson, K. W., Jones, B., & Peng, R. D. (2018). Projected trends in high-mortality heatwaves under different scenarios of climate, population, and adaptation in 82 US communities. *Climatic Change*, *146*(3–4), 455–470. https://doi.org/10.1007/s10584-016-1779-x

Bady, M. (2014). Analysis of outdoor human thermal comfort within three major cities in Egypt. *Open Access Library Journal*, *1*, e457. https://doi.org/10.4236/oalib.1100457

Bartzokas, A., Lolis, C. J., Kassomenos, P. A., & McGregor, G. R. (2013). Climatic characteristics of summer human thermal discomfort in Athens and its connection to atmospheric circulation. *Natural Hazards and Earth System Sciences*, *13*(12), 3271–3279. https://doi.org/10.5194/nhess-13-3271-2013

Bourbonnais, R., Zayed, J., Lévesque, M., Busque, M. A., Duguay, P., & Truchon, G. (2013). Identification of workers exposed concomitantly to heat stress and chemicals. *Industrial Health*, *51*(1), 25–33. https://doi.org/10.2486/indhealth.2012-0095

Ceccherini, G., Russo, S., Ameztoy, I., Marchese, A. F., & Carmona-Moreno, C. (2017). Heat waves in Africa 1981–2015, observations and reanalysis. *Natural Hazards and Earth System Sciences*, *17*(1), 115–125. https://doi.org/10.5194/nhess-17-115-2017

Chen, K., Horton, R. M., Bader, D. A., Lesk, C., Jiang, L., Jones, B., et al. (2017). Impact of climate change on heat-related mortality in Jiangsu Province, China. *Environmental pollution*, *224*, 317–325. https://doi.org/10.1016/j.envpol.2017.02.011

Dee, D. P., Uppala, S. M., Simmons, A. J., Berrisford, P., Poli, P., Kobayashi, S., & Vitart, F. (2011). The ERA-Interim reanalysis: Configuration and performance of the data assimilation system. *Quarterly Journal of the Royal Meteorological Society*, *137*, 553–597. http://doi.org/10.1002/qj.828

Diallo, I., Bain, C. L., Gaye, A. T., Moufouma-Okia, W., Niang, C., Dieng, M. D., & Graham, R. (2014). Simulation of the West African monsoon onset using the HadGEM3-RA regional climate model. *Climate Dynamics*, *43*(3–4), 575–594. https://doi.org/10.1007/s00382-014-2219-0

Diallo, I., Sylla, M. B., Giorgi, F., Gaye, A. T., & Camara, M. (2012). Multi-model GCM-RCM ensemble based projections of temperature and precipitation over West Africa for the early 21st century. *International Journal of Geophysics*, *2012*, 1–19. https://doi.org/10.1155/2012/972896

Diffenbaugh, N. S., Pal, J. S., Giorgi, F., & Gao, X. (2007). Heat stress intensification in the Mediterranean climate change hotspot. *Geophysical Research Letters*, *34*, L11706. https://doi.org/10.1029/2007GL030000

Dosio, A. (2017). Projection of temperature and heat waves for Africa with an ensemble of CORDEX regional climate models. *Climate Dynamics*, *49*(1–2), 493–519. https://doi.org/10.1007/s00382-016-3355-5

Dosio, A., Mentaschi, L., Fischer, E. M., & Wyser, K. (2018). Extreme heat waves under 1.5 °C and 2 °C global warming. *Environmental Research Letters*, *13*(5), 054006.

Dosio, A., Panitz, H.-J., Schubert-Frisius, M., & Luethi, D. (2015). Dynamically downscaling of CMIP5 CGMs over CORDEX-Africa with COSMO-CLM: Analysis of the added value over the present climate. *Climate Dynamics*, *44*, 2637–2661. https://doi.org/10.1007/s00382-015-2664-4

Epstein, Y., & Moran, D. S. (2006). Thermal comfort and the heat stress indices. *Industrial Health*, *44*(3), 388–398. https://doi.org/10.2486/indhealth.44.388

Faye, B., Webber, H., Naab, J., MacCarthy, D. S., Adam, M., Ewert, F., et al. (2018). Impacts of 1.5 versus 2.0°C on cereal yields in the West African Sudan Savanna. *Environmental Research Letters*, *13*, 034014. https://doi.org/10.1088/1748-9326/aaab40

Fontaine, B., Janicot, S., & Monerie, P. A. (2013). Recent changes in air temperature, heat waves occurrences, and atmospheric circulation in Northern Africa. *Journal of Geophysical Research: Atmospheres*, *118*, 8536–8552. https://doi.org/10.1002/jgrd.50667

Gasparrini, A., Guo, Y., Sera, F., Vicedo-Cabrera, A. M., Huber, V., Tong, S., et al. (2017). Projections of temperature-related excess mortality under climate change scenarios. *The Lancet Planetary Health*, *1*(9), e360–e367. https://doi.org/10.1016/S2542-5196(17)30156-0

Ghani, S., Bialy, E. M., Bakochristou, F., Gamaledin, S. M. A., Rashwan, M. M., & Hughes, B. (2017). Thermal comfort investigation of an outdoor air-conditioned area in a hot and arid environment. *Science and Technology for the Built Environment*, *23*(7), 1113–1131. https://doi.org/10.1080/23744731.2016.1267490

Giles, B. D., Balafoutis, C., & Maheras, P. (1990). Too hot for comfort: the heatwaves in Greece in 1987 and 1988. *International Journal of Biometeorology*, *34*(2), 98–104. https://doi.org/10.1007/BF01093455

Giorgi, F., Coppola, E., Raffaele, F., Diro, G. T., Fuentes-Franco, R., Giuliani, G., et al. (2014). Changes in extremes and hydroclimatic regimes in the CREMA ensemble projections. *Climatic Change*, *125*(1), 39–51. https://doi.org/10.1007/s10584-014-1117-0

Giorgi, F., & Bi, X. (2005). Regional changes in surface climate interannual variability for the 21st century from ensembles of global model simulations. *Geophysical Research Letters*, *32*, L13701. https://doi.org/10.1029/2005GL023002

Giorgi, F., & Gutowski, W. J. Jr. (2015). Regional dynamical downscaling and the CORDEX initiative. *Annual Review of Environment and Resources*, *40*, 467–490. https://doi.org/10.1146/annurev-environ-102014-021217

Giorgi, F., Jones, C., & Asrar, G. (2009). Addressing climate information needs at the regional level: The CORDEX framework. *Bulletin World Meteorological Organization*, *58*, 175–183.

Harris, I. P. D. J., Jones, P. D., Osborn, T. J., & Lister, D. H. (2014). Updated high-resolution grids of monthly climatic observations–the CRU TS3.10 dataset. *International Journal of Climatology*, *34*(3), 623–642. https://doi.org/10.1002/joc.3711

Im, E. S., Pal, J. S., & Eltahir, E. A. (2017). Deadly heat waves projected in the densely populated agricultural regions of South Asia. *Science Advances*, *3*(8), e1603322.

Intergovernmental Panel on Climate Change (2014). *Regional aspects (Africa). Climate change 2014: Summary for policy makers. Synthesis Report*, (p. 32). Geneva: Intergovernmental Panel on Climate Change (IPCC).

James, R., & Washington, R. (2013). Changes in African temperature and precipitation associated with degrees of global warming. *Climatic Change*, *117*, 859–872. https://doi.org/10.1007/s10584-012-0581-7

Kalnay, E., Kanamitsu, M., Kistler, R., Collins, W., Deaven, D., Gandin, L., et al. (1996). The NCEP/NCAR 40-year reanalysis project. *Bulletin of the American Meteorological Society*, *77*(3), 437–471. https://doi.org/10.1175/1520-0477(1996)077%3C0437:TNYRP%3E2.0.CO;2

Kjellstrom, T., Holmer, I., & Lemke, B. (2009). Workplace heat stress, health and productivity—An increasing challenge for low and middle-income countries during climate change. *Global Health Action*, *2*(1), 2047. https://doi.org/10.3402/gha.v2i0.2047

Klutse, N. A. B., Ajayi, V. O., Gbobaniyi, E. O., Egbebiyi, T. S., Kouadio, K., Nkrumah, F., et al. (2018). Potential impact of 1.5°C and 2°C global warming on consecutive dry and wet days over West Africa. *Environmental Research Letters*, *13*, 055013. https://doi.org/10.1088/1748-9326/aab37b

Lawrimore, J. H., Menne, M. J., Gleason, B. E., Williams, C. N., Wuertz, D. B., Vose, R. S., & Rennie, J. (2011). An overview of the Global Historical Climatology Network monthly mean temperature data set, version 3. *Journal of Geophysical Research*, *116*, D19121. https://doi.org/10.1029/2011JD016187

Lee, D., & Brenner, T. (2015). Perceived temperature in the course of climate change: An analysis of global heat index from 1979 to 2013. *Earth System Science Data*, *7*(2), 193–202. https://doi.org/10.5194/essd-7-193-2015

Lee, J. Y., & Kim, H. (2016). Projection of future temperature-related mortality due to climate and demographic changes. *Environment International*, *94*, 489–494. https://doi.org/10.1016/j.envint.2016.06.007

Liang, C., Zheng, G., Zhu, N., Tian, Z., Lu, S., & Chen, Y. (2011). A new environmental heat stress index for indoor hot and humid environments based on Cox regression. *Building and Environment*, *46*(12), 2472–2479. https://doi.org/10.1016/j.buildenv.2011.06.013

Linares, C., Mirón, I. J., Montero, J. C., Criado-Álvarez, J. J., Tobías, A., & Díaz, J. (2014). The time trend temperature–mortality as a factor of uncertainty analysis of impacts of future heat waves. *Environmental Health Perspectives*, *122*(5), A118. https://doi.org/10.1289/ehp.1308042

Liu, Z., Anderson, B., Yan, K., Dong, W., Liao, H., & Shi, P. (2017). Global and regional changes in exposure to extreme heat and the relative contributions of climate and population change. *Scientific Reports*, *7*, 43909. https://doi.org/doi:10.1038/srep43909

Lucas, R. A., Epstein, Y., & Kjellstrom, T. (2014). Excessive occupational heat exposure: A significant ergonomic challenge and health risk for current and future workers. *Extreme Physiology & Medicine*, *3*(1), 14. https://doi.org/10.1186/2046-7648-3-14

Mensah, E., Almas, L. K., Guerrero, B. L., Lust, D. G., & Ibrahimov, M. (2016). Agriculture and the state of food insecurity in western Africa. In *2016 Annual Meeting*, *February 6–9*, *2016*, *San Antonio*, *Texas* (No. 229976). Southern *Agricultural Economics* Association.

Mora, C., Dousset, B., Caldwell, I. R., Powell, F. E., Geronimo, R. C., Bielecki, C. R., et al. (2017). Global risk of deadly heat. *Nature Climate Change*, *7*(7), 501–506. https://doi.org/10.1038/nclimate3322

Moss, R. H., Edmonds, J. A., Hibbard, K. A., Manning, M. R., Rose, S. K., Van Vuuren, D. P., et al. (2012). The next generation of scenarios for climate change research and assessment. *Nature*, *463*, 747–756. https://doi.org/10.1038/nature08823

Nikiema, P. M., Sylla, M. B., Ogunjobi, K., Kebe, I., Gibba, P., & Giorgi, F. (2017). Multi-model CMIP5 and CORDEX simulations of historical summer temperature and precipitation variabilities over West Africa. *International Journal of Climatology*, *37*(5), 2438–2450. https://doi.org/10.1002/joc.4856

Nikulin, G., Lennard, C., Dosio, A., Kjellström, E., Chen, Y., Hänsler, A., et al. (2018). The effects of 1.5 and 2 degrees of global warming on Africa in the CORDEX ensemble. *Environmental Research Letters*, *13*, 065003. https://doi.org/10.1088/1748-9326/aab1b1

National Institute for Occupational Safety and Health (2016). NIOSH criteria for a recommended standard: Occupational exposure to heat and hot environments. By Jacklitsch B, Williams WJ, Musolin K, Coca A, Kim J-H, Turner N. Cincinnati, OH: U.S. Department of Health and Human Services, Centers for Disease Control and Prevention, National Institute for Occupational Safety and Health, DHHS (NIOSH) Publication 2016–106.

Oleson, K. W., Anderson, G. B., Jones, B., McGinnis, S. A., & Sanderson, B. (2015). Avoided climate impacts of urban and rural heat and cold waves over the U.S. using large climate model ensembles for RCP8.5 and RCP4.5. *Climatic Change*, *146*(3–4), 377–392.

Pal, J. S., & Eltahir, E. A. (2016). Future temperature in southwest Asia projected to exceed a threshold for human adaptability. *Nature Climate Change*, *6*(2), 197–200. https://doi.org/10.1038/nclimate2833

Perkins-Kirkpatrick, S. E., & Gibson, P. B. (2017). Changes in regional heatwave characteristics as a function of increasing global temperature. *Scientific Reports*, *7*(1), 12256. https://doi.org/10.1038/s41598-017-12520-2

Poupkou, A., Nastos, P., Melas, D., & Zerefos, C. (2011). Climatology of discomfort index and air quality index in a large urban Mediterranean agglomeration. *Water, Air, & Soil Pollution*, *222*(1–4), 163–183. https://doi.org/10.1007/s11270-011-0814-9

Ropo, O. I., Perez, M. S., Werner, N., & Enoch, T. I. (2017). Climate variability and heat stress index have increasing potential ill-health and environmental impacts in the east London. *South Africa. International Journal of Applied Engineering Research*, *12*(17), 6910–6918.

Rothfusz, L. P. (1990). The heat index equation (or, more than you ever wanted to know about heat index). *Fort Worth*, *Texas: National Oceanic and Atmospheric Administration*, *National Weather Service*, *Office of Meteorology*, *9023*.

Russo, S., Dosio, A., Graversen, R. G., Sillmann, J., Carrao, H., Dunbar, M. B., et al. (2014). Magnitude of extreme heat waves in present climate and their projection in a warming world. *Journal of Geophysical Research: Atmospheres*, *119*, 12,500–12,512. https://doi.org/10.1002/2014JD022098

Russo, S., Marchese, A. F., Sillmann, J., & Immé, G. (2016). When will unusual heat waves become normal in a warming Africa? *Environmental Research Letters*, *11*(5), 054016. https://doi.org/10.1088/1748-9326/11/5/054016

Schleussner, C. F., Lissner, T. K., Fischer, E. M., Wohland, J., Perrette, M., Golly, A., et al. (2016). Differential climate impacts for policy-relevant limits to global warming: The case of 1.5 ° C and 2 ° C. *Earth System Dynamics*, *7*, 327–351. https://doi.org/10.5194/esd-7-327-2016

Sohar, E., Adar, R., & Kaly, J. (1963). Comparison of the Industrial Health 2006, 44, 388–398 environmental heat load in various parts of Israel. *Bulletin of the Research Council of Israel*, *10E*, 111–5.

Steadman, R. G. (1979). The assessment of sultriness. Part I: A temperature-humidity index based on human physiology and clothing science. *Journal of Applied Meteorology*, *18*(7), 861–873. https://doi.org/10.1175/1520-0450(1979)018%3C0861:TAOSPI%3E2.0.CO;2

Sultan, B., & Gaetani, M. (2016). Agriculture in West Africa in the twenty-first century: Climate change and impacts scenarios, and potential for adaptation. *Frontiers in Plant Science*, *7*, 1262. https://dx.doi.org/10.3389%2Ffpls.2016.01262

Sylla, M. B., Elguindi, N., Giorgi, F., & Wisser, D. (2016). Projected robust shift of climate zones over West Africa in response to anthropogenic climate change for the late 21st century. *Climatic Change*, *134*, 241–253. https://doi.org/10.1007/s10584-015-1522-z

Sylla, M. B., Nikiema, M., Gibba, P., Kebe, I., & Klutse, N. A. B. (2016). Climate change over West Africa: Recent trends and future projections. In J. A. Yaro, & J. Hesselberg (Eds.), *Adaptation to climate change and variability in rural West Africa* (pp. 25–40). Cham: Springer. https://doi.org/10.1007/978-3-319-31499-0_3

Takahashi, K., Honda, Y., & Emori, S. (2007). Assessing mortality risk from heat stress due to global warming. *Journal of risk research*, *10*(3), 339–354. https://doi.org/10.1080/13669870701217375

Thom, E. C. (1959). The discomfort index. *Weatherwise*, *12*, 59–60.

Yousif, T. A., & Tahir, H. M. (2013). Application of Thom's thermal discomfort index in Khartoum state, Sudan. *Journal of Forest Products and Industries*, *2*(5), 36–38.

Zougmoré, R., Partey, S., Ouédraogo, M., Omitoyin, B., Thomas, T., Ayantunde, A., et al. (2016). Toward climate-smart agriculture in West Africa: A review of climate change impacts, adaptation strategies and policy developments for the livestock, fishery and crop production sectors. *Agriculture & Food Security*, *5*(1), 26. https://doi.org/10.1186/s40066-016-0075-3